

## ARTICLE OPEN



# Increased VH4+JH6+ antibody heavy chain use in plasmablasts from asymptomatic multiple sclerosis patients

Sara Benavides<sup>1,8</sup>, Scott Christley<sup>1,2,8</sup>, Kiel M. Telesford<sup>1</sup>, Chad Smith<sup>1</sup>, Katelyn Sheffer<sup>1</sup>, Yipin Wu<sup>1</sup>, Wei Zhang<sup>1</sup>, Key M. Tse<sup>1</sup>, Hannah J. Greenberg<sup>1</sup>, Morgan Jackson<sup>1</sup>, Caitlin Chapman<sup>1</sup>, Darina Dinov<sup>1</sup>, Paula Hardeman<sup>1</sup>, Aksel Siva<sup>3</sup>, Daniel Pelletier<sup>4</sup>, Orhun Kantarci<sup>5</sup>, Christine Lebrun-Frénay<sup>6</sup>, Lindsay G. Cowell<sup>2</sup>, Darin T. Okuda<sup>1</sup> and Nancy L. Monson<sup>1,7</sup>✉

© The Author(s) 2026

Radiologically isolated syndrome (RIS) is a neurological condition in people with demyelinating lesions on brain and/or spinal cord magnetic resonance imaging (MRI) studies, but without clinical symptoms of disease. Elucidating the immune profile of people with RIS (pwRIS) who will display MRI or clinical features of advancing disease is critical to our understanding of disease pathogenesis. Our lab previously identified features of B cell dysregulation in people with clinically isolated syndrome (pwCIS), who have both demyelinating lesions and a first clinical event of disease. The goal of this study was to compare features of B cell dysregulation in pwRIS, pwCIS, and healthy controls (HC). The second goal was to determine if these features of B cell dysregulation would be evident in people who meet the new MS diagnostic criteria, particularly in the context of their disease course for 5 years post-sampling. Features of plasmablast responses that distinguish pwRIS from pwCIS include PB expansion, antigen-driven selection, VH4 and JH6 antibody gene over-usage, neuron reactivity by purified IgG and individually cloned antibodies. Furthermore, VH4:JH6 pairing in plasmablasts was higher in people with stable MS who do not show changes in MRI or clinical events from those with advancing disease activity.

*Genes & Immunity*; <https://doi.org/10.1038/s41435-026-00389-z>

## INTRODUCTION

Radiologically isolated syndrome (RIS) represents the earliest detectable pre-clinical phase of multiple sclerosis (MS) for some patients, [1–5] punctuated by abnormal and incidentally found demyelinating lesions within the brain and/or spinal cord from MRI studies [1, 4–6]. In contrast, people diagnosed with clinically isolated syndrome (pwCIS) initially present with both clinical symptoms and 2 or more lesions by MRI. Prior to the newly released 2024 MS diagnosis criteria [7], a second demyelinating clinical event or evidence of dissemination in time on MRI would be required to achieve a diagnosis of MS, which occurs in 63% of pwCIS over the subsequent 4.3 years since the initial presentation [8]. In contrast, the risk for a first demyelinating clinical event in people with RIS (pwRIS) is estimated at 34% within 5 years of RIS diagnosis using the 2009 criteria, which increases to 51% at 10 years [2, 4, 5, 9].

Early treatments with disease-modifying therapies (DMTs) are thought to reduce future demyelinating clinical events in pwRIS [9–11] and pwCIS [9–13]. The new diagnostic criteria will allow for many pwRIS and pwCIS to be diagnosed with MS, allowing for approved treatments to be administered earlier within the disease spectrum. However, up to 49% of pwRIS will not develop clinical symptoms of MS [1, 5], and distinguishing which individuals with RIS will experience disease advancement is an

important aspect of providing optimal care for this vulnerable population. In pwRIS, features resulting in a higher risk for a first demyelinating clinical event within 5 years include younger age at time of evaluation (<37 years), male sex, and presence of spinal cord lesions. [1, 3, 14]. Others have also demonstrated that biological markers, including the presence of unique cerebrospinal-fluid (CSF) restricted oligoclonal bands (OCBs) [15], CSF- and serum-derived neurofilament light (NfL) concentrations [16–19] could be useful in stratifying individuals likely to advance to a clinically defined demyelinating disease course of MS.

In examining the potential role of B cells in the disease course of MS, we determined that plasmablasts (PBs), a subset of highly differentiated, early antibody secreting B cells (ASCs) [20], represent a significant proportion of the B cell pool in the CSF of people with MS (pwMS) [21]. Others have shown the frequency of ASCs correlates with the extent of gray matter disease by MRI [21]. Our laboratory previously demonstrated that pwCIS who advance to a diagnosis of MS using the 2017 McDonald criteria [4] display an expansion of PBs expressing antibody heavy chain rearrangements of the variable heavy 4 (VH4) family in the CSF [21] and blood [21, 22]. We have also demonstrated antibodies utilizing VH4 family genes cloned from PBs in the CSF of pwMS or in the blood of pwCIS who advance to MS diagnosis are enriched

<sup>1</sup>Department of Neurology, UT Southwestern Medical Center, Dallas, TX, USA. <sup>2</sup>School of Public Health, UT Southwestern Medical Center, Dallas, TX, USA. <sup>3</sup>Department of Neurology, Istanbul University Cerrahpaşa School of Medicine, Istanbul, Turkey. <sup>4</sup>NeuroRX Research, Montreal, QC, Canada. <sup>5</sup>Neurology, Mayo Clinic, Rochester, MN, USA. <sup>6</sup>Neurology MS Clinic Nice, Pasteur 2 University Hospital; UR2CA-URRIS, Côte d'Azur University, Nice, France. <sup>7</sup>Department of Immunology, UT Southwestern Medical Center, Dallas, TX, USA. <sup>8</sup>These authors contributed equally: Sara Benavides, Scott Christley. ✉email: [nancy.monson@utsouthwestern.edu](mailto:nancy.monson@utsouthwestern.edu)

Received: 19 May 2025 Revised: 2 February 2026 Accepted: 18 February 2026

Published online: 19 March 2026

for binding to neurons [22, 23]. Others have also shown plasmablast expansion [21, 24–26], VH4 overuse [27–29], and neuron binding by VH4+ antibodies cloned from B cells of pwMS [21, 22, 30, 31]. In this study, we sought to determine if this B cell profile of increased PB frequency and VH4 overuse was also evident in pwRIS who present with brain inflammation characteristic of MS, but without clinical symptoms. To do this, we compared the PB profile in the blood of pwRIS, pwCIS and HC by 1) frequency, 2) immunogenetics, and 3) antibody reactivity. We found that VH4 family use was significantly higher in pwRIS compared to pwCIS. VH4+ antibodies cloned from PBs of pwRIS displayed a higher frequency of neuron reactivity compared to non-VH4+ antibodies (as we had observed in pwCIS). Joint heavy gene 6 (JH6) use was also significantly higher in pwRIS compared to pwCIS, culminating in increased VH4 to JH6 pairing use by PBs from pwRIS compared to pwCIS and more importantly, in people with stable MS who do not show changes in MRI or clinical events for 5 years post-sampling.

## MATERIALS AND METHODS

### Ethics approval and consent to participate

All subjects and/or their legally authorized study partners signed the written informed consent (STU022011-211) approved by the Institutional Review Board of the UT Southwestern Medical Center (UTSW), in accordance with the Federal-wide Assurance on file with the Department of Health and Human Services (USA). All methods were performed in accordance with guidelines and regulations by these entities.

### Patient information and sample procurement

Demographic and clinical data for the cohort (Table 1) are provided. Subjects that comprise the RIS cohort were originally enrolled in the ARISE study to evaluate the efficacy of dimethyl fumarate (DMF) to delay clinical symptom onset [10]. Inclusion criteria for the ARISE trial were that subjects must meet the 2009 RIS criteria including incidental anomalies identified on MRI of the brain or spinal cord from an evaluation unrelated to MS. These subjects also had no clinically apparent neurological symptoms at the time of trial entry. However, 12/33 (36%) of the RIS subjects had a first clinical event within 5 years of trial entry with an average time to first event of 12.9 months. Samples from RIS subjects for this study were collected at baseline prior to randomization of the cohort in the ARISE trial and had not been exposed to any disease-modifying therapies at that time. No samples were collected prior to study enrollment. Samples from CIS subjects for this study were collected at the time of their first clinical demyelinating event and had not been exposed to disease-modifying therapies at that time. Samples were processed through the UTSW Neuroscience Biorepository [32, 33]. After collection, peripheral blood mononuclear cells (PBMCs) were isolated and stored as previously described [34]. The MS group consists of those RIS and CIS subjects who meet the 2024 revised McDonald criteria for MS diagnosis ( $n = 28$  for RIS and  $n = 19$  for CIS).

### Flow cytometry for immune profiling B cell subsets

Participants' PBMC cells were removed from cryostasis and stained for CD19, CD27, and CD38 as previously described [35]. Briefly, a BD FACSAria V cell sorter was used to sort CD19+CD27++CD38+ plasmablast B cells either in bulk for B cell receptor (BCR) genetics studies or as single cells in 96-well plates for recombinant antibody generation. The staining protocol used the following antibodies from BD Biosciences CD27-FITC, CD38-APC, CD19-BV421, CD4-PE-Cy7, CD8-PE, anti-CD20-PerCP-Cy5.5, CD45-APC-Cy7, CD56-PE-Cy5, CD3-V500, CD14-AF500, and HLA-DR-BV711. After sorting, the single cells were flash frozen on dry ice and stored at  $-80^{\circ}\text{C}$  for future analysis as previously established by our laboratory [22, 36].

### BCR library preparation and sequencing

Genomic DNA (gDNA) was isolated from bulk-sorted plasmablast B cells using DNeasy Blood and Tissue kit (Qiagen). The PCR product was amplified using Qiagen Multiplex PCR kit (Qiagen). We used B-cell receptor gene rearrangement primer sets and conditions previously published by others [37]. Nextera UD Index Primers (IDT) were added to the amplicons and were purified using AMPure XP beads (Beckman Coulter). Barcoded

libraries were pooled and loaded onto an Illumina MiSeq instrument using MiSeq Reagent Kit v3 (Illumina) at the UTSW genomics sequencing core.

### Antibody sequence analysis

Sequences were analyzed using the VDJServer analysis portal as previously described [38–41].

### Recombinant human Ab (rhAb) cloning, expression, and purification

The variable domains of the recombinant antibodies of heavy chains and light chains from individually sorted antigen-experienced CD19+CD27++CD38+ plasmablast B cells were amplified with multiple rounds of PCR as previously described [21, 22, 42]. Resultant rearrangements were synthesized (Integrated DNA Technologies) and cloned as previously described [22, 43] with modifications to use FreeStyle CHO-S (Chinese Hamster Ovary) cells (Invitrogen) for production.

### Purification of IgG from plasma and neuron binding by flow cytometry and immunocytochemistry

We employed protein G chromatography (Cytiva Life Sciences) and detection of binding by flow cytometry [26] and immunocytochemistry [26, 30] as previously described. Coverslips were visualized on a Zeiss Axioscan 7 fluorescent slide scanner with a 20x/0.8NA air objective lens.

### Quantification of autoreactivity by rhAbs

Autoreactivity of rhAbs was quantified using a custom-written Fiji macro [44]. In brief, nuclei and cellular outlines were determined and added to the Region of Interest (ROI) manager. Then, the cytoplasmic mean fluorescence intensity (MFI) of positively-stained cells was measured while excluding potential non-specific antibody aggregates. Finally, the MFI of the background (regions where no cells were detected) was subtracted from these values.

### Statistical analysis

Graphpad Prism 10 software was used to perform statistical analyses. One-way ANOVA was performed to examine results comparing 3 groups. For any comparisons with only 2 groups, Welch's *T*-test was used due to the unequal sample size. The Shapiro–Wilk normality test was used to identify datasets with bimodal distributions and in those cases where the dataset did not pass the normality test, the mean of the group was used to divide the group dataset into high and low designations.

## RESULTS

### Plasmablasts are expanded in pwRIS, pwCIS and pwMS

We previously demonstrated that a high frequency of PBs in the blood indicates ongoing active inflammation prominent in individuals experiencing a clinical demyelinating event of MS [21, 22]. To determine if PBs are expanded in pwRIS who do not display clinical manifestations of disease but do display brain lesions typical of MS, the frequency of PB (CD19+CD27++CD38+) in the blood was determined by flow cytometry. Figure 1A shows pwRIS has an average frequency of 3.58% PBs in blood, which is significantly higher than the frequency of PBs in HCs (1.08%). Similarly, pwCIS, who manifest a first clinical demyelinating event, have an average frequency of 3.03% PBs in the blood, a finding significantly higher when compared to HCs, but similar to pwRIS. Next, we applied the new 2024 MS diagnostic criteria (pwMS) to the pwRIS and pwCIS subjects and found that 47 of the 57 subjects (82.5%) met the 2024 revised McDonald criteria for MS diagnosis. Figure 1B shows pwMS have an average frequency of 3.06% PBs in blood, which is significantly higher than the frequency of PBs in HCs (1.08%). We also employed a new approach [26] to examine neuron-binding potential within the purified IgG (plgG) antibody pool from serum samples (Fig. 1C, D) and found that pwMS had a significantly higher frequency of plgG that bound a human neuronal cell line by flow cytometry compared to plgG from HC (4.36% vs 3.03%,  $p = 0.0001$ ) (Fig. 1E).

**Table 1.** Baseline demographic and clinical information.

	HC <sup>a</sup>	RIS <sup>b,c</sup>	CIS <sup>c,d</sup>	MS <sup>c,e</sup>	Advancing <sup>f</sup>	Stable <sup>g</sup>
N <sup>h</sup>	39	33	26	47	38	21
Average age in years	42	44	39	42	40	46
Standard deviation	13.9	14.82	12.30	13.14	13.326	14.33
Sex, %	49%	61%	69%	64%	63%	67%
Female	41%	39%	31%	36%	37%	33%
Male	10%	0%	0%	0%	0%	0%
Unknown						
Race, %	64%	91%	69%	83%	76%	90%
White	0%	6%	12%	9%	11%	5%
Black or African American	36%	3%	19%	9%	13%	5%
Unknown						
Ethnicity, %	8%	9%	4%	6%	5%	10%
Hispanic	54%	91%	77%	87%	82%	90%
Non-Hispanic	38%	0%	19%	6%	13%	0%
Unknown						
Average EDSS score	N/A	0	1.71	0.06	0.85	0
Oligoclonal bands, %	N/A	76%	80%	89%	79%	76%
Brain lesions on MRI, %	N/A	12%	16%	17%	11%	19%
Gadolinium enhancement T2 lesions	N/A	100%	68%	96%	76%	100%
Spinal cord lesions on MRI, %	N/A	55%	85%	66%	76%	52%
Number (%) with clinical event	N/A	12 (36%) <sup>i</sup>	26 (100%) <sup>j</sup>	19 (40%) <sup>ij</sup>	38 (100%) <sup>ij</sup>	N/A

HC Healthy Control, RIS Radiologically Isolated Syndrome, CIS Clinically Isolated Syndrome, EDSS Expanded Disability Status Scale.

<sup>a</sup>Individuals defined as healthy are sex and age matched to the cohort.

<sup>b</sup>Individuals fulfilling 2009 RIS Criteria were also enrolled in the ARISE trial [11].

<sup>c</sup>24 of the 26 CIS subjects in the cohort were not on DMTs at the time of sample collection.

<sup>d</sup>Individuals experiencing a first demyelinating event, placing them at high risk for evolution to MS were categorized as clinically isolated syndrome (CIS) according to the 2017 McDonald criteria. Sampling was done at the time of the first demyelinating event.

<sup>e</sup>pwRIS ( $n = 28$ )/pwCIS ( $n = 19$ ) who fulfill the 2024 revised McDonald criteria for MS diagnosis.

<sup>f</sup>pwRIS ( $n = 12$ )/pwCIS ( $n = 26$ ) who meet criteria for "Advanced", defined as having a clinical event within 5 years of sampling.

<sup>g</sup>pwRIS ( $n = 21$ )/pwCIS ( $n = 0$ ) who meet criteria for "Stable", defined as having no clinical event within 5 years of sampling.

<sup>h</sup>Some demographic and/or clinical data were not available for all subjects. Subject level data are included in Supplemental Data.

<sup>i</sup>Within 5 years post-sampling.

<sup>j</sup>At time of sampling.

### Expansion of VH4 family and individual VH4 genes by PBs from pwRIS

The RIS cohort displayed a higher frequency of PBs compared to HC (Fig. 1), which may manifest as discordance in antibody variable heavy chain (VH) family or individual gene usage. To address this, we calculated the frequency of VH family usage in bulk-sorted PBs of all subjects in the 3 groups (HC, RIS and CIS). The VH family genes are divided into 7 families according to gene homology [45]. The frequency of usage for VH families by group is shown in Fig. 2A. The RIS group displayed an expansion of VH family 4 (VH4) usage compared to CIS ( $p = 0.005$ ) (Fig. 2B). Comparison of VH4 family usage by the HC group to RIS (Fig. 2A) or to MS (Fig. 2C) was not significant. To determine whether particular VH4 genes were driving the higher frequency of VH4 usage in RIS compared to CIS, we analyzed the frequency of use in each of the 10 major genes within the VH4 family. VH4-34, VH4-39, and VH4-59 use was significantly higher in RIS compared to CIS (Fig. 2D). Of note, overuse of these 3 VH4 genes was observed for several RIS subjects (Fig. 2E–G).

### VH4+ antibodies from pwRIS are enriched for reactivity to human neurons

Plasmablasts from pwCIS have a propensity to express VH4+ antibodies that bind neurons [22]. To determine the frequency of PBs expressing neuron-binding antibodies within the RIS cohort, we cloned 63 antibodies expressed by individual PBs sorted from

the blood of pwRIS. The rhAbs cloned were from 12 RIS subjects that displayed high PB frequency and ranged from 4–6 rhAbs cloned per subject (Table 2). Six of the major VH4 genes were included in the RIS rhAb cohort with representation of all 6 JH segments. 52 of the rhAbs were VH4+ with an average homology of 94.5% (average range 90–100%). For comparison, 11 VH3+ rhAbs were cloned from the RIS cohort with an average homology of 93.11% (average range 83.04–98.44%). We tested the ability of the rhAbs to bind a human neuroblastoma cell line, SH-Sy5y, using flow cytometry (Fig. 3). The gating strategy for experiments using this approach is provided in Fig. 1C, D. The average percentage of VH3+ rhAbs binding to SH-Sy5y was 3.66% (Fig. 3A), whereas the average percentage of VH4+ rhAbs binding to SH-Sy5y was 13.06% (Fig. 3A). Of the top 20% rhAbs that bound SH-Sy5y in this assay, all 12 utilized VH4 genes with somatic hypermutation (SHM) accumulation across the spectrum (Table 3). We used immunocytochemistry (ICC) of SH-Sy5y cells to query the frequency and staining patterns of the neuron-binding VH4+ rhAbs (Fig. 3B, Supplementary Fig. 1 and Supplementary Table 1). The majority of RIS-derived rhAbs bind targets residing in the cytoplasm of SH-Sy5y cells.

### Expansion of JH6 use by PBs from pwRIS

The antibody heavy chain variable domain rearrangement consists of a variable (VH) gene, a D (DH) segment, and a joining (JH) gene. There are 6 JH genes, of which JH4 is most often used. Since 5 of

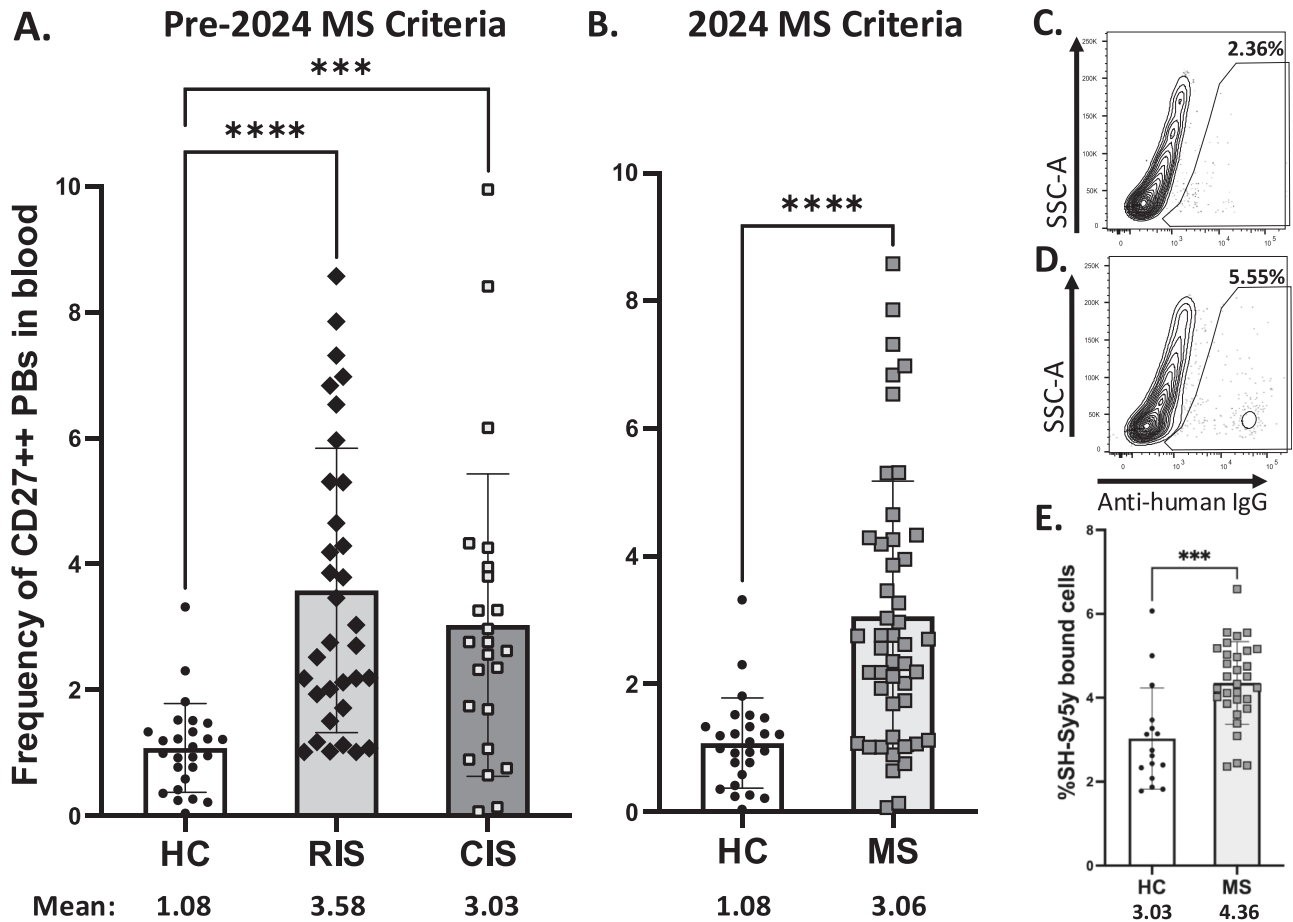


**Fig. 1 Plasmablasts are expanded in pwRIS, pwCIS, and pwMS.** The frequency of PBs in the blood of HC ( $n = 26$ ), vs pwRIS ( $n = 33$ ), vs pwCIS ( $n = 24$ ) (A) was determined by flow cytometry. The averages of each group are depicted as a bar graph, and the mean values are provided below the X-axis. The ANOVA  $p$ -value for (A) was  $<0.0001$ . Panel B is the frequency of PBs in the blood of the same HC group vs the 2024 revised McDonald criteria for MS diagnosis (pwMS;  $n = 47$ ) for those pwRIS and pwCIS subjects that meet this criteria. The averages of each group are depicted as a bar graph, and the mean values are provided below the X-axis. The gating strategy to determine the frequency of purified IgG binding to the human neuroblastoma cell line, SH-Sy5y, is shown in (C) for a sample considered negative, and (D) for a sample considered positive. The frequency of purified IgG binding for HC vs pwMS is shown in (E) ( $p = 0.0002$ ). Each data point represents an individual research participant in (A, B, E). \*\*\*\* $p = 0.0001$ ; \*\*\* $p = 0.0002$ .

the top 12 neuron-binding VH4+ rHabs used JH6 genes (Table 3), we asked whether JH gene use was also discordant in the RIS group. To do this, we queried the bulk sorted PB antibody heavy chain repertoire datasets for JH gene use (Supplementary Fig. 1 and Fig. 4). All 3 groups (HC, RIS, and CIS) use JH4 most frequently, followed by JH6 (Supplementary Fig. 1A). However, the RIS cohort displayed an expansion of JH6 use compared to the CIS cohort (Fig. 4A), resulting in a reduced JH4:JH6 ratio in RIS compared to HC and CIS (Fig. 4B). The JH6 gene includes two additional codons, and so its use can oftentimes skew the CDR3 length and charge. The CDR3 length of PBs expressing variable domains that include JH6 was predictably longer than non-JH6 users (Supplementary Fig. 1B), but the CDR3 charge of JH6 users compared to non-JH6 users was no different (Supplementary Fig. 1C, D).

#### Expansion of VH4 to JH6 pairing use by PBs from pwRIS and those with stable MS

Considering that individual VH4 family genes and JH6 gene usage were increased in RIS compared to CIS, we examined the repertoire for overuse of VH4 to JH6 pairing (VH4+JH6+; Fig. 4). Indeed, we found that the frequency of VH4+JH6+ pairs was higher in RIS compared to CIS (7.52 vs 5.22,  $p < 0.05$ ) (Fig. 4C). We did not observe an increase in VH4+JH6+ pair use in MS compared to HC (data not shown). Of note, the VH4+JH6+ frequency in RIS

was bimodal ( $p = 0.047$  by Shapiro–Wilk normality test) such that the RIS<sub>low</sub> ( $n = 15$ ) had a similar VH4+JH6+ frequency compared to CIS. The RIS<sub>high</sub> ( $n = 15$ ) had an increased frequency of VH4+JH6+ use compared to CIS ( $p = 0.0001$ ). Since 20 of the 47 subjects in the MS group did not have clinical symptoms during the 5 years of monitoring after sample collection, we asked whether the increase in VH4+JH6+ pair use was more prominent in those subjects without clinical symptoms (labeled as “stable”) than those subjects that manifest clinical symptoms (labeled as “advancing”) within the MS group. Indeed, VH4+JH6+ pair use was significantly increased in pwMS that did not display clinical symptoms compared to those that did in the 5 years post-sampling ( $p = 0.007$ ) (Fig. 4D, E).

#### DISCUSSION

PBs and the antibodies they produce are a central component of the neuropathology of MS. This is evidenced by 1) expansion of PBs in the CSF of pwCIS who evolve to MS [21, 22, 24]; 2) the strong correlation between PB or antibody levels in pwMS with brain gray matter atrophy [21, 22, 46] and disability [47] among pwMS, and 3) the success of disease-modifying therapies among pwMS that reduce B cell frequencies [21, 22, 24], including PBs. In addition, at the time of a first clinical demyelinating event, PB

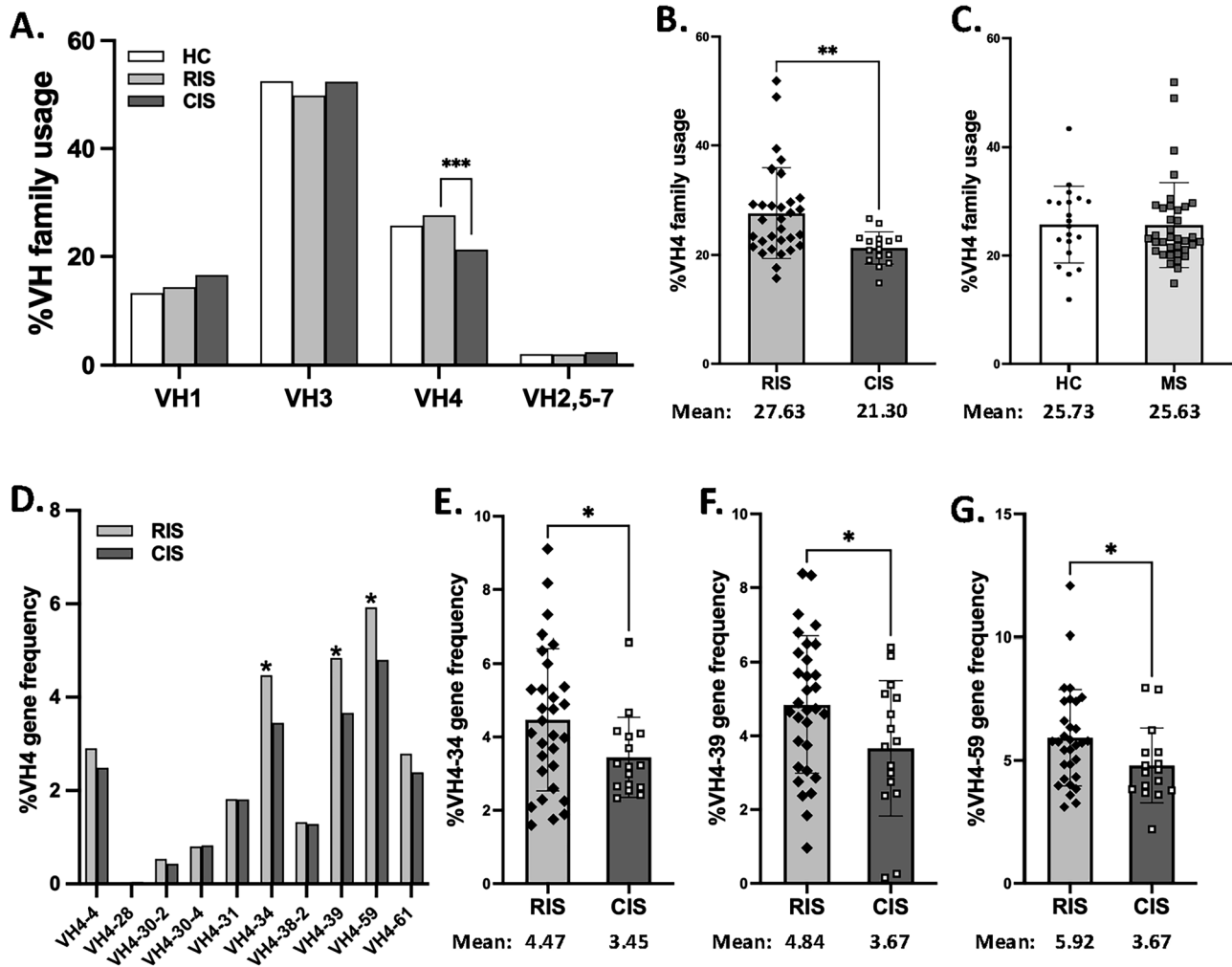


**Fig. 2** Expansion of VH4 family and individual VH4 genes by PBs from pwRIS. Variable heavy chain family usage for families 1–7 was calculated for each subject of HC ( $n = 20$ ), vs pwRIS ( $n = 31$ ), vs pwCIS ( $n = 16$ ) (A). The white bars represent HC, the middle light gray bars represent RIS, and the dark gray bars represent CIS. The ANOVA,  $p$ -value for VH4 use in (A) was  $p = 0.0006$ . VH4 family use of the RIS and CIS groups per subject are shown in (B). VH4 family use of the HC ( $n = 20$ ) and MS ( $n = 36$ ) groups per subject are shown in (C). Individual VH4 gene frequencies of the RIS and CIS groups are shown in (D). Individual VH4 gene frequencies of VH4-34, VH4-39, and VH4-59 are shown in (E–G), respectively, for the RIS and CIS groups. \*\* $p = 0.005$ ; \* $p < 0.05$ .

**Table 2.** Cloning summary by RIS subject.

	Total cloned	Total VH4 (%)	AVE homology
RIS-01	6	4 (66.67)	97.19
RIS-03	5	3 (60.00)	92.18
RIS-09	5	4 (80.00)	92.16
RIS-15	5	5 (100.00)	95.94
RIS-17	6	6 (100.00)	91.01
RIS-18	5	3 (60.00)	96.00
RIS-19	5	4 (80.00)	94.92
RIS-20	4	2 (50.00)	90.58
RIS-22	6	6 (100.00)	95.92
RIS-33	6	6 (100.00)	95.03
RIS-34	5	4 (80.00)	96.93
TOTAL	63	52 (82.54)	94.54

frequencies are elevated in the blood when the first clinical attack occurs and will continue to rise if the subject remains untreated [22]. Our focus here was to compare features of PB biology in individuals presenting with brain inflammation characteristic of MS, without (pwRIS) and with (pwCIS) clinical demyelinating events at the time of sampling. Of note, prior studies using flow cytometry to characterize the immune profile within the spectrum of neurodegenerative disease, including MS, have not focused on pwRIS [21, 22, 24, 48, 49], and to our knowledge this is the first study examining both pwRIS and pwCIS that meet the 2024 MS diagnostic criteria [7].

We found the frequency of PBs in the blood was similar in pwRIS and pwCIS, and both groups were expanded in comparison to HC. These data suggest PB expansion in the blood is a feature common to subjects presenting with brain inflammation characteristic of MS. PB expansion is also independent of clinical demyelinating manifestations of disease, as only the pwCIS group (and not the pwRIS group) is characterized by clinical demyelinating events and a spectrum of Expanded Disability Status Scale scores. PB expansion is also extended to subjects within the pwRIS and pwCIS groups that meet the 2024 MS diagnostic criteria compared to HC. We had previously noted people with early and

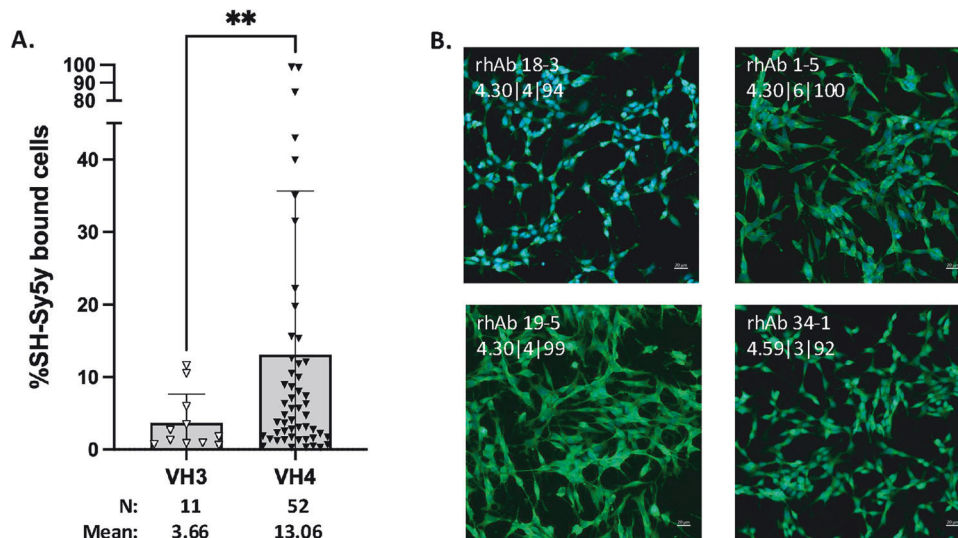


**Fig. 3** **VH4+ antibodies from pwRIS are enriched for reactivity to human neurons.** **A** Comparison of the percentage of RIS-derived VH3+ or VH4+ recombinant human antibodies binding to SH-Sy5y cells. Each data point represents an individual rhAb, the number of rhAbs is indicated below the x-axis, followed by the mean of each group. The Welch's *t*-test *p*-value for **(A)** is *p* = 0.007 as indicated by \*\*. **B** Illustrates intracellular binding patterns observed by anti-neuronal rhAbs from the RIS cohort by immunostaining of the human neuroblastoma SH-Sy5y cell line. The top left line indicates the rhAb name, and the bottom left line indicates the VH4 gene usage, the JH segment, and the percent homology to the germline of that particular rhAb. Scale bar: 20 μm. Green: rhAb. Blue: DAPI nuclear stain.

**Table 3.** Immunogenetics of Top 20% rhAbs that bind SH-Sy5y by flow cytometry.

rhAb name	VH family	%binding	%Homology	VH:JH usage
RIS34-1	VH4	12.60	92.51	VH4-59:JH3
RIS13-5	VH4	15.30	99.57	VH4-39:JH5
RIS33-2	VH4	15.60	93.01	VH4-61:JH6
RIS18-1	VH4	19.70	96.52	VH4-59:JH1
RIS01-5	VH4	22.20	100.00	VH4-30:JH6
RIS01-1	VH4	31.45	90.22	VH4-04:JH6
RIS18-3	VH4	35.00	94.04	VH4-30:JH4
RIS22-5	VH4	39.93	100.00	VH4-34:JH6
RIS13-2	VH4	42.95	95.22	VH4-34:JH4
RIS19-1	VH4	84.70	89.94	VH4-61:JH3
RIS19-5	VH4	98.30	99.20	VH4-30:JH4
RIS01-6	VH4	98.70	100.00	VH4-61:JH6

VH variable heavy, VH:JH usage variable heavy (VH) and joining heavy (JH) gene segment usage.

established MS were more likely to display PB expansion if they presented with spinal cord lesions [21]. As both the pwRIS and pwCIS groups here display a prevalence of spinal cord lesions (55% and 85%, respectively), PB expansion in both groups was likely predictable based on our earlier findings. Of note, the frequency of spinal cord lesions in this cohort remains comparable to the average of 80% in pwMS [50, 51] and 30–68% in pwCIS [52, 53]. One early study reported that PB frequency was no different in 12 pwRIS compared to HC [54]. The prevalence of spinal cord lesions within that pwRIS group was not reported, but based on our multiple observations that spinal cord lesion prevalence is related to PB expansion, it was likely reduced. Further elucidation of this finding in the future would benefit from inclusion of pwRIS with prevalence of brain lesions. Of note, the impact of race and ethnicity on PB expansion could not be evaluated in this cohort, as the majority of the pwRIS and pwCIS subjects were non-Hispanic white females. Others have demonstrated PB expansion in Black or African American subjects with

MS [26, 49], although examination of spinal cord lesion prevalence was not addressed. No information is available regarding PB expansion in Hispanic subjects with MS. Future studies should be done to further elucidate the connection between spinal cord lesion prevalence and PB expansion, inclusive of race and ethnicity diversity.

We considered that PB expansion in both pwRIS and pwCIS would be reflected in the skewing of antibody gene expression. In previous reports by us and others, variable heavy chain family 4 (VH4) use was increased in the cerebrospinal fluid (CSF) and blood of pwCIS and pwMS [21, 22, 27, 28, 42]. Yet here we observed that VH4 use in blood-derived PB of pwRIS, pwCIS, and in subjects that meet the 2024 revised McDonald criteria for MS diagnosis was similar to that observed in blood-derived PB of HC. There are at least two possible reasons for this discrepancy from earlier studies. First, these earlier studies by others compared the antibody repertoires of pwCIS and pwMS groups to expected germline frequencies, which do not account for repertoire changes

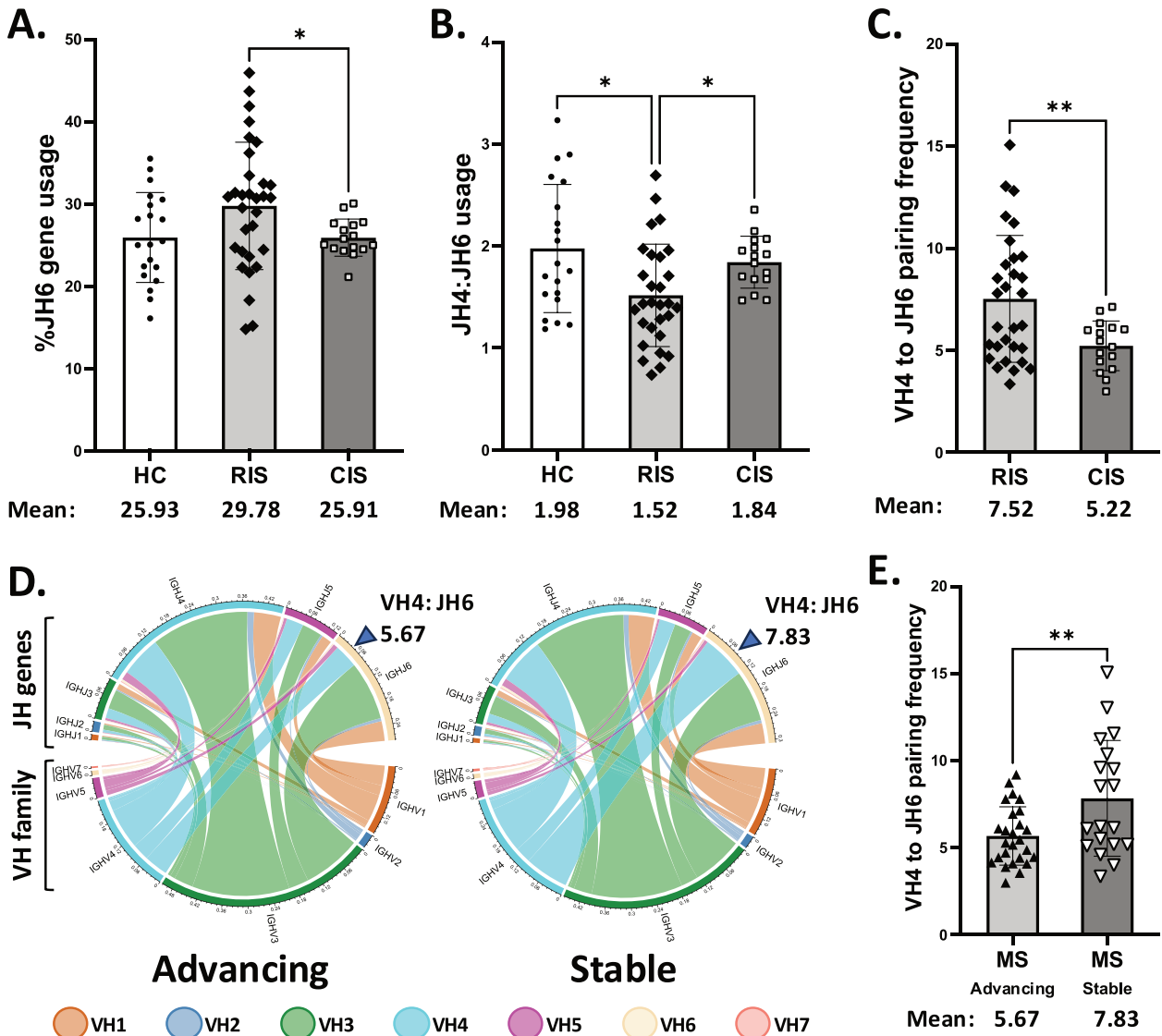


**Fig. 4** Expansion of JH6 and VH4 to JH6 pairing frequency by PBs from pwRIS and those with stable disease. **A** JH6 frequency for each subject in HC, pwRIS, and pwCIS. **B** The JH4:JH6 ratio for each subject in HC, pwRIS, and pwCIS. **C** The VH4 to JH6 pairing frequency for each subject in HC, pwRIS, and pwCIS. **D** Ribbon plots displaying the frequency of VH families 1–7 pairing to each JH gene in the Advancing MS vs Stable MS groups. Each ribbon color depicts a particular VH family as indicated. The frequency value of VH4 pairing to JH6 is indicated for the Advancing vs Stable groups. **E** Individual VH4 to JH6 pairing frequencies. HC,  $n = 20$ ; RIS,  $n = 31$  for (A, C), and  $n = 29$  for (B); CIS,  $n = 16$ ; Advancing MS,  $n = 26$ ; Stable MS,  $n = 19$ . The ANOVA for (A) was 0.0177 and the ANOVA for (B) was  $<0.0001$ . \* $p < 0.05$ ; \*\* $p < 0.01$ .

emerging from antigen exposure. In our earlier studies, we compared the antibody repertoires of CSF-derived repertoires to blood-derived CD19+ B cells from HC rather than expected germline frequencies. However, our earlier approach to the analysis did not account for repertoire changes in the context of antigen exposure dependent on the compartment from which the B cell was isolated. To address rigor in the current study, we used PBs isolated from the blood of healthy controls as the comparator population, controlling for B cell subtype, compartment origin (blood), and demographics when available. The second possible reason for the discrepancy from earlier studies is that the technology used to generate antibody gene repertoires in these early reports demonstrating VH4 over-use in CSF and blood of pwCIS and pwMS was single cell PCR (scPCR), which surveyed on average 46 cells per subject repertoire. Here, we used Next Generation Sequencing (NGS), which produced 416-fold more cells per repertoire than by scPCR with an average of 19,143 PBs per subject repertoire.

We did observe, however, VH4 family use was higher in blood-derived PBs from pwRIS compared to pwCIS. We sought to understand the potential impact of VH4 expansion in pwRIS by determining if VH4+ antibodies expressed by PBs from pwRIS bind neurons. We previously documented that VH4+ PBs from pwCIS are both expanded and enriched for autoreactivity towards neurons [22]. To examine the autoreactive nature of VH4+ PBs in pwRIS, we cloned 52 VH4+ rhAbs and 11 VH3+ rhAbs as controls and demonstrated that 44% and 56% of antibodies expressed by VH4+ PB bind the human neuroblastoma cell line, SH-Sy5y by flow cytometry or ICC respectively. In comparison, of the 30 VH4+ PB-derived antibodies we cloned from pwCIS previously, 60% ( $n = 18$ ) bound to SH-Sy5y cells by ICC [22]. Thus, the frequency of VH4+ PBs producing anti-neuronal antibodies was similar in pwCIS compared to pwRIS (60% vs 56%). One limitation of this comparison is that the antibodies we cloned from the CIS group previously were enriched for SHM accumulation, whereas the antibodies we cloned from the RIS group here were a

mixture of antibodies that were either positive or negative for SHM accumulation. When the RIS antibody panel is restricted to those antibodies that accumulated SHM ( $n = 37$ ), the frequency of anti-neuronal binding remains similar at 57% (21 of 37). Thus, while VH4 family gene use and high SHM increase the likelihood of neuron binding properties, other antibody gene features not considered here (such as CDR3 composition and specific antigen target binding properties) are likely to impact binding as well.

VH4-34, VH4-39, and VH4-59 use was specifically increased in PBs of pwRIS compared to pwCIS, and these 3 VH4 genes were frequently used by neuron-binding VH4+ RIS rhAbs. In studies of antibody selection in healthy controls, B cells expressing VH4-34 antibodies are often autoreactive and therefore suppressed from use within the antigen-exposed repertoire [55, 56]. Here, we found that VH4-34+ antibodies are autoreactive as defined by their ability to bind neurons, but rather than VH4-34 use being suppressed in the repertoire, VH4-34+ PBs from pwRIS are expanded. We also found that VH4-39+ PBs and VH4-59+ PBs are neuron reactive and expanded in pwRIS. Previous studies report over-use of VH4-34 and VH4-39 in MS brain tissue [29, 57], and both VH4-39 and VH4-59 in MS-derived CSF [31]. While these other studies did not examine neuronal reactivity by antibodies utilizing these particular VH4 genes, we would predict they would bind neurons. We interpret these findings in aggregate to indicate VH4+ PBs (particularly those using VH4-34, -39, and -59 genes) are neuron reactive and detected early in the blood of pwRIS. Reduction of these gene frequencies in the blood of pwCIS and increased frequencies of these VH4 genes in the CSF and brain tissue of well-established pwMS likely indicate matriculation of certain VH4+ PB from the blood to the CNS may be an indicator of MS disease progression. Future studies should include examination of the impact antibodies using particular antibody genes have on neuron health, which have been limited to date [58–60].

The likely explanation for the expansion of VH4+ PB producing antibodies that bind neurons is founded in mechanistic defects within the immune system designed to suppress B cell autoreactivity in MS [48]. Of note, autoreactivity in this early work was defined by binding to multiple antigens, including double stranded DNA, insulin, and LPS, with confirmed binding to myelin-enriched brain lysate. Our data extends this concept to suggest autoreactivity checkpoint defects are also evident in pwRIS, allowing for expansion of VH4+ PBs, particularly those using VH4-34, VH4-39, and VH4-59 genes with a high likelihood of neuron autoreactivity. Determining the impact of neuron-reactive VH4+ antibodies on the course of MS disease (RIS vs CIS, for example) would be of particular interest. Identification of the neuronal antigen targets would be required for such experiments, but was not done here. Of note, the neuronal staining patterns of rhAbs from pwRIS and pwCIS are similar in that they tend to bind intracellular antigen targets rather than surface antigen targets. Current dogma has been that the cellular localization of the target antigen determines the pathological potential of the autoantibody, such that most pathological autoantibodies bind extracellular targets, not intracellular targets [61]. However, more recent examples indicate that some autoantibodies recognizing intracellular targets can be pathogenic [62, 63]. In either case, targeting B cells expressing antibodies using particular VH4 genes [64] may have utility in this context.

Finally, the 2024 revised McDonald criteria for MS diagnosis would include most, if not all pwRIS and allow them access to therapies approved for use in the treatment of MS. However, many pwRIS will never advance to display clinical evidence of demyelination [1, 3, 14], and would unlikely benefit from DMTs that primarily reduce relapse rates. Thus, our second goal was to examine PB antibody repertoires from within the cohort for features that may distinguish subjects with advancing versus stable disease over the next 5 years post-sampling. Indeed, we found an increased frequency of VH4 to JH6 pairing within the PB

antibody repertoires of pwRIS who had stable disease for the next 5 years post-sampling. One confounder to the antibody repertoire analysis, including VH4 to JH6 pairing frequency, is the integrity of the blood-brain barrier (BBB). The BBB is designed to limit lymphocyte trafficking to the central nervous system (CNS), but is frequently compromised in pwMS due to extensive neuroinflammation in the CNS [65, 66]. Thus, BBB integrity is likely higher in people with stable disease, which would result in the blood acting as a “sink” for lymphocytes that would normally traffic to the CNS, which could be detected as changes in PB frequency and/or antibody genetics. Biomarkers of BBB breakdown are beginning to emerge across neurodegenerative conditions [65, 67] and may facilitate our understanding of blood-derived VH4+JH6+ PB expansion in the context of BBB integrity among people with stable MS disease.

In conclusion, we have found that PBs are expanded in people with demyelinating lesions within the brain and/or spinal cord from magnetic resonance imaging (MRI) studies, even in those subjects that do not display clinical symptoms of disease. Analysis of antibody genetics using deep sequencing of the repertoires indicated that PBs using VH4 antibody heavy chain genes were expanded in pwRIS compared to pwCIS, which was driven by particular use of VH4-34, VH4-39, and VH4-59 genes within the VH4 family. VH4+ PBs from both pwRIS and pwCIS are most likely to bind neurons than VH3+ PBs and also tend to accumulate somatic hypermutations at a high rate. These data are consistent with previous studies that B cells from pwMS escape mechanisms designed to suppress autoreactivity [48] and further extend these studies to include neuron autoreactivity. We also found that the VH4 to JH6 pairing frequency was increased in PBs of pwMS who remain stable 5 years post-sampling, compared to pwMS subjects who display disease progression during the 5 years post-sampling. To our knowledge, this is the first antibody genetics biomarker associated with disease stability in MS. However, the study is limited in that the impact of VH4+JH6+ antibodies produced by PBs from pwRIS on neurodegeneration associated with MS disease progression was not addressed. Factors that may have also influenced the results included the high prevalence of spinal cord lesions within the cohort and variation in BBB integrity. Future studies should examine the impact of these factors on the B cell profile reported here and the role of anti-neuronal antibodies in the mechanism of neuroinflammation associated with MS.

## DATA AVAILABILITY

The AIRR-seq data is available in the AIRR Data Commons at VDJServer Community Data Portal with UUID: aa4b61e3-2809-4a47-bcf5-d09a82618851.

## REFERENCES

- Lebrun-Frenay C, Rollot F, Mondot L, Zephir H, Louapre C, Le Page E, et al. Risk factors and time to clinical symptoms of multiple sclerosis among patients with radiologically isolated syndrome. *JAMA Netw Open*. 2021;4:e2128271.
- Lebrun-Frenay C, Okuda DT, Siva A, Landes-Chateau C, Azevedo CJ, Mondot L, et al. The radiologically isolated syndrome: revised diagnostic criteria. *Brain*. 2023;146:3431–43.
- Okuda DT, Siva A, Kantarci O, Inglese M, Katz I, Tutuncu M, et al. Radiologically isolated syndrome: 5-year risk for an initial clinical event. *PLoS One*. 2014;9:e90509.
- Thompson AJ, Banwell BL, Barkhof F, Carroll WM, Coetzee T, Comi G, et al. Diagnosis of multiple sclerosis: 2017 revisions of the McDonald criteria. *Lancet Neurol*. 2018;17:162–73.
- Okuda DT, Mowry EM, Beheshtian A, Waubant E, Baranzini SE, Goodin DS, et al. Incidental MRI anomalies suggestive of multiple sclerosis: the radiologically isolated syndrome. *Neurology*. 2009;72:800–5.
- Okuda DT, Mowry EM, Cree BA, Crabtree EC, Goodin DS, Waubant E, et al. Asymptomatic spinal cord lesions predict disease progression in radiologically isolated syndrome. *Neurology*. 2011;76:686–92.
- Montalban X. 2024 Revisions to McDonald Diagnostic Criteria for Multiple Sclerosis [Video]. In: Presented atECTRIMS Congress in Copenhagen. Scientific

- Session 1: New Diagnostic Criteria. Copenhagen, Denmark:ECTRIMS; 2024. Available from: <https://www.neurologylive.com/view/2024-revisions-mcdonald-diagnostic-criteria-multiple-sclerosis-peter-calabresi>.
8. Kuhle J, Disanto G, Dobson R, Adiatori R, Bianchi L, Topping J, et al. Conversion from clinically isolated syndrome to multiple sclerosis: a large multicentre study. *Mult Scler*. 2015;21:1013–24.
  9. Lebrun-Frenay C, Siva A, Sormani MP, Landes-Chateau C, Mondot L, Bovis F, et al. Teriflunomide and time to clinical multiple sclerosis in patients with radiologically isolated syndrome: the TERIS randomized clinical trial. *JAMA Neurol*. 2023;80:1080–8.
  10. Okuda DT, Kantarci O, Lebrun-Frenay C, Sormani MP, Azevedo CJ, Bovis F, et al. Dimethyl fumarate delays multiple sclerosis in radiologically isolated syndrome. *Ann Neurol*. 2023;93:604–14.
  11. Okuda DT, Azevedo CJ, Pelletier D, Moog TM, Moazami S, Rezvani S, et al. Dimethyl fumarate preserves brainstem and cervical spinal cord integrity in radiologically isolated syndrome. *J Neurol*. 2024;271:5899–910.
  12. Miller AE, Wolinsky JS, Kappos L, Comi G, Freedman MS, Olsson TP, et al. Oral teriflunomide for patients with a first clinical episode suggestive of multiple sclerosis (TOPIC): a randomised, double-blind, placebo-controlled, phase 3 trial. *Lancet Neurol*. 2014;13:977–86.
  13. Longbrake EE, Cross AH, Salter A. Efficacy and tolerability of oral versus injectable disease-modifying therapies for multiple sclerosis in clinical practice. *Mult Scler J Exp Transl Clin*. 2016;2:2055217316677868.
  14. Lebrun-Frenay C, Kantarci O, Siva A, Sormani MP, Pelletier D, Okuda DT, et al. Radiologically isolated syndrome: 10-year risk estimate of a clinical event. *Ann Neurol*. 2020;88:407–17.
  15. Dobson R, Ramagopalan S, Davis A, Giovannoni G. Cerebrospinal fluid oligoclonal bands in multiple sclerosis and clinically isolated syndromes: a meta-analysis of prevalence, prognosis and effect of latitude. *J Neurol Neurosurg Psychiatry*. 2013;84:909–14.
  16. Rival M, Galoppin M, Thouvenot E. Biological markers in early multiple sclerosis: the paved way for radiologically isolated syndrome. *Front Immunol*. 2022;13:866092.
  17. Bielekova B, Pranzatelli MR. Promise, progress, and pitfalls in the search for central nervous system biomarkers in neuroimmunological diseases: a role for cerebrospinal fluid immunophenotyping. *Semin Pediatr Neurol*. 2017;24:229–39.
  18. Zamecnik CR, Sowa GM, Abdelhak A, Dandekar R, Bair RD, Wade KJ, et al. An autoantibody signature predictive for multiple sclerosis. *Nat Med*. 2024;30:1300–8.
  19. Bjornevik K, Cortese M, Healy BC, Kuhle J, Mina MJ, Leng Y, et al. Longitudinal analysis reveals high prevalence of Epstein-Barr virus associated with multiple sclerosis. *Science*. 2022;375:296–301.
  20. Nutt SL, Hodgkin PD, Tarlinton DM, Corcoran LM. The generation of antibody-secreting plasma cells. *Nat Rev Immunol*. 2015;15:160–71.
  21. Ligocki AJ, Rounds WH, Cameron EM, Harp CT, Frohman EM, Courtney AM, et al. Expansion of CD27high plasmablasts in transverse myelitis patients that utilize VH4 and JH6 genes and undergo extensive somatic hypermutation. *Genes Immun*. 2013;14:291–301.
  22. Rivas JR, Ireland SJ, Chkheidze R, Rounds WH, Lim J, Johnson J, et al. Peripheral VH4+ plasmablasts demonstrate autoreactive B cell expansion toward brain antigens in early multiple sclerosis patients. *Acta Neuropathol*. 2017;133:43–60.
  23. Ligocki AJ, Rivas JR, Rounds WH, Guzman AA, Li M, Spadaro M, et al. A distinct class of antibodies may be an indicator of gray matter autoimmunity in early and established relapsing remitting multiple sclerosis patients. *ASN Neuro*. 2015;7:1759091415609613.
  24. Cepok S, Rosche B, Grummel V, Vogel F, Zhou D, Sayn J, et al. Short-lived plasma blasts are the main B cell effector subset during the course of multiple sclerosis. *Brain*. 2005;128:1667–76.
  25. Bogers L, Engelenburg HJ, Janssen M, Unger PA, Melief MJ, Wierenga-Wolf AF, et al. Selective emergence of antibody-secreting cells in the multiple sclerosis brain. *EBioMedicine*. 2023;89:104465.
  26. Telesford KM, Smith C, Mettlen M, Davis MB, Cowell L, Kittles R, et al. Neuron-binding antibody responses are associated with Black ethnicity in multiple sclerosis during natalizumab treatment. *Brain Commun*. 2023;5:fcad218.
  27. Bennett JL, Haubold K, Ritchie AM, Edwards SJ, Burgoon M, Shearer AJ, et al. CSF IgG heavy-chain bias in patients at the time of a clinically isolated syndrome. *J Neuroimmunol*. 2008;199:126–32.
  28. Owens GP, Wings KM, Ritchie AM, Edwards S, Burgoon MP, Lehnhoff L, et al. VH4 gene segments dominate the intrathecal humoral immune response in multiple sclerosis. *J Immunol*. 2007;179:6343–51.
  29. Owens GP, Kraus H, Burgoon MP, Smith-Jensen T, Devlin M E, Gilden DH. Restricted use of VH4 germline segments in an acute multiple sclerosis brain. *Ann Neurol*. 1998;43:236–43.
  30. Zhang W, Joshi C, Smith C, Ujas TA, Rivas JR, Cowell L, et al. Neuronal binding by antibodies can be influenced by low pH stress during the isolation procedure. *J Immunol Methods*. 2023;521:113535.
  31. von Budingen HC, Kuo TC, Sirota M, van Belle CJ, Apeltsin L, Glanville J, et al. B cell exchange across the blood-brain barrier in multiple sclerosis. *J Clin Invest*. 2012;122:4533–43.
  32. Estrada K, Whelan CW, Zhao F, Bronson P, Handsaker RE, Sun C, et al. A whole-genome sequence study identifies genetic risk factors for neuromyelitis optica. *Nat Commun*. 2018;9:1929.
  33. Li J, Bazzi SA, Schmitz F, Tanno H, McDaniel JR, Lee CH, et al. Molecular level characterization of circulating aquaporin-4 antibodies in neuromyelitis optica spectrum disorder. *Neurol Neuroimmunol Neuroinflamm*. 2021;8:e1034.
  34. Smith C, Telesford KM, Piccirillo SGM, Licon-Munoz Y, Zhang W, Tse KM, et al. Astrocytic stress response is induced by exposure to astrocyte-binding antibodies expressed by plasmablasts from pediatric patients with acute transverse myelitis. *J Neuroinflammation*. 2024;21:161.
  35. Monson NL, Ireland SJ, Ligocki AJ, Chen D, Rounds WH, Li M, et al. Elevated CNS inflammation in patients with preclinical Alzheimer's disease. *J Cereb Blood Flow Metab*. 2014;34:30–3.
  36. Jacobi AM, Mei H, Hoyer BF, Mumtaz IM, Thiele K, Radbruch A, et al. HLA-DRhigh/CD27high plasmablasts indicate active disease in patients with systemic lupus erythematosus. *Ann Rheum Dis*. 2010;69:305–8.
  37. Rosenfeld AM, Meng W, Chen DY, Zhang B, Granot T, Farber DL, et al. Computational evaluation of B-cell clone sizes in bulk populations. *Front Immunol*. 2018;9:1472.
  38. Christley S, Scarborough W, Salinas E, Rounds WH, Toby IT, Fonner JM, et al. VDJServer: a cloud-based analysis portal and data commons for immune repertoire sequences and rearrangements. *Front Immunol*. 2018;9:976.
  39. Ye J, Ma N, Madden TL, Ostell JM. IGBLAST: an immunoglobulin variable domain sequence analysis tool. *Nucleic Acids Res*. 2013;41:W34–40.
  40. Gupta NT, Vander Heiden JA, Uduman M, Gadala-Maria D, Yaari G, Kleinstein SH. Change-O: a toolkit for analyzing large-scale B cell immunoglobulin repertoire sequencing data. *Bioinformatics*. 2015;31:3356–8.
  41. Zar JH. *Biostatistical analysis*, 5th ed. Upper Saddle River, NJ: Prentice Hall/Pearson; 2010. p. 644.
  42. Cameron EM, Spencer S, Lazarini J, Harp CT, Ward ES, Burgoon M, et al. Potential of a unique antibody gene signature to predict conversion to clinically definite multiple sclerosis. *J Neuroimmunol*. 2009;213:123–30.
  43. Tiller T, Meffre E, Yurasov S, Tsuiji M, Nussenzweig MC, Wardemann H. Efficient generation of monoclonal antibodies from single human B cells by single cell RT-PCR and expression vector cloning. *J Immunol Methods*. 2008;329:112–24.
  44. Schindelin J, Arganda-Carreras I, Frise E, Kaynig V, Longair M, Pietzsch T, et al. Fiji: an open-source platform for biological-image analysis. *Nat Methods*. 2012;9:676–82.
  45. Kohsaka H, Carson DA, Rassenti LZ, Ollier WE, Chen PP, Kittles TJ, et al. The human immunoglobulin V(H) gene repertoire is genetically controlled and unaltered by chronic autoimmune stimulation. *J Clin Invest*. 1996;98:2794–800.
  46. Boziki M, Bakirtzis C, Sintila SA, Kesidou E, Gounari E, Ioakimidou A, et al. Ocrelizumab in patients with active primary progressive multiple sclerosis: clinical outcomes and immune markers of treatment response. *Cells*. 2022;11:1959.
  47. Gasperi C, Salmen A, Antony G, Bayas A, Heesen C, Kumpfel T, et al. Association of intrathecal immunoglobulin G synthesis with disability worsening in multiple sclerosis. *JAMA Neurol*. 2019;76:841–9.
  48. Kinnunen T, Chamberlain N, Morbach H, Cantaert T, Lynch M, Preston-Hurlburt P, et al. Specific peripheral B cell tolerance defects in patients with multiple sclerosis. *J Clin Invest*. 2013;123:2737–41.
  49. Telesford KM, Kaunzner UW, Perumal J, Gauthier SA, Wu X, Diaz I, et al. Black African and Latino/a identity correlates with increased plasmablasts in MS. *Neurol Neuroimmunol Neuroinflamm*. 2020;7:e634.
  50. Kreiter D, Postma AA, Hupperts R, Gerlach O. Hallmarks of spinal cord pathology in multiple sclerosis. *J Neurol Sci*. 2024;456:122846.
  51. Bot JC, Barkhof F, Polman CH, Lycklama A, Nijeholt GJ, de Groot V, et al. Spinal cord abnormalities in recently diagnosed MS patients: added value of spinal MRI examination. *Neurology*. 2004;62:226–33.
  52. Sombecke MH, Wattjes MP, Balk LJ, Nielsen JM, Vrenken H, Uitdehaag BM, et al. Spinal cord lesions in patients with clinically isolated syndrome: a powerful tool in diagnosis and prognosis. *Neurology*. 2013;80:69–75.
  53. Arrambide G, Rovira A, Sastre-Garriga J, Tur C, Castillo J, Rio J, et al. Spinal cord lesions: a modest contributor to diagnosis in clinically isolated syndromes but a relevant prognostic factor. *Mult Scler*. 2018;24:301–12.
  54. Guerrier T, Labalette M, Launay D, Lee-Chang C, Outtertyck O, Lefevre G, et al. Proinflammatory B-cell profile in the early phases of MS predicts an active disease. *Neurol Neuroimmunol Neuroinflamm*. 2018;5:e431.
  55. Schickel JN, Glauzy S, Ng YS, Chamberlain N, Massad C, Isnardi I, et al. Self-reactive VH4-34-expressing IgG B cells recognize commensal bacteria. *J Exp Med*. 2017;214:1991–2003.
  56. Pugh-Bernard AE, Silverman GJ, Cappione AJ, Villano ME, Ryan DH, Insel RA, et al. Regulation of inherently autoreactive VH4-34 B cells in the maintenance of human B cell tolerance. *J Clin Invest*. 2001;108:1061–70.

57. Baranzini SE, Jeong MC, Butunoi C, Murray RS, Bernard CC, Oksenberg JR. B cell repertoire diversity and clonal expansion in multiple sclerosis brain lesions. *J Immunol.* 1999;163:5133–44.
58. Liu Y, Given KS, Harlow DE, Matschulat AM, Macklin WB, Bennett JL, et al. Myelin-specific multiple sclerosis antibodies cause complement-dependent oligodendrocyte loss and demyelination. *Acta Neuropathol Commun.* 2017;5:25.
59. Peschl P, Schanda K, Zeka B, Given K, Bohm D, Ruprecht K, et al. Human antibodies against the myelin oligodendrocyte glycoprotein can cause complement-dependent demyelination. *J Neuroinflammation.* 2017;14:208.
60. Hoftberger R, Lassmann H, Berger T, Reindl M. Pathogenic autoantibodies in multiple sclerosis - from a simple idea to a complex concept. *Nat Rev Neurol.* 2022;18:681–8.
61. Sechi E, Flanagan EP. Antibody-mediated autoimmune diseases of the CNS: challenges and approaches to diagnosis and management. *Front Neurol.* 2021;12:673339.
62. Racanelli V, Prete M, Musaraj G, Dammacco F, Perosa F. Autoantibodies to intracellular antigens: generation and pathogenetic role. *Autoimmun Rev.* 2011;10:503–8.
63. Salapa HE, Thibault PA, Libner CD, Ding Y, Clarke JWE, Denomy C, et al. hnRNP A1 dysfunction alters RNA splicing and drives neurodegeneration in multiple sclerosis - from a simple idea to a complex concept. *Nat Commun.* 2024;15:356.
64. Paliwal S, Thakkar D, Chin WJ, Lee W, Neo JY, Tay L, et al. Selective targeting of pathogenic auto-reactive VH4–34 B cells with a rationally developed anti-VH4–34 antibody offers a new therapeutic approach for autoimmune disorders. *J Immunol.* 2023;210:238.20–20.
65. Janigro D, Bailey DM, Lehmann S, Badaut J, O'Flynn R, Hirtz C, et al. Peripheral Blood and Salivary Biomarkers of Blood-Brain Barrier Permeability and Neuronal Damage: Clinical and Applied Concepts. *Front Neurol.* 2020;11:577312.
66. Takata F, Nakagawa S, Matsumoto J, Dohgu S. Blood-Brain Barrier Dysfunction Amplifies the Development of Neuroinflammation: Understanding of Cellular Events in Brain Microvascular Endothelial Cells for Prevention and Treatment of BBB Dysfunction. *Front Cell Neurosci.* 2021;15:661838.
67. Merlini M, Sozmen EG, Subramanian KS, Nana AL, Seeley WW, Akassoglou K. Three-Dimensional Imaging of Fibrinogen and Neurovascular Alterations in Alzheimer's Disease. *Methods Mol Biol.* 2023;2561:87–101.

## ACKNOWLEDGEMENTS

We would like to thank the patients and healthy subjects who participated in these studies; without you, this wouldn't be possible! We thank all the clinical staff at UTSW associated with the Neuroscience Biorepository (Director, Dr. Ben Greenberg) for their assistance in sample acquisition and transport. The authors also thank the Children's Medical Research flow core for the use of their flow cytometry instrumentation and expertise, the Whole Brain Microscopy Facility (Director, Dr. Denise Ramirez) for the use of their Zeiss AxioScanner 7 imaging technology, and the Quantitative Light Microscopy Core (Director, Dr. Marcel Mettlen) for helping with image analysis. Special thanks to Denny and Sandy Miller for the use of their retreat home to write this paper.

## AUTHOR CONTRIBUTIONS

Conceptualization: NL. Methodology: SB, SC, Kiel MT, CS, HJG, WZ, YW, Key MT, KS, MJ, LGC. Investigation: SB, SC, Kiel MT, CS, CC, DD, PH. Visualization: SB, SC, Kiel MT, CS,

HJG, NLM. Funding acquisition: NLM. Project administration: NLM. Supervision: NLM. Writing – original draft: SB, NLM. Writing – review & editing: SB, SC, Kiel MT, CS, HJG, WZ, YW, Key MT, AS, DP, OK, CLF, LGC, DTO, NLM

## FUNDING

National Institutes of Health grant NS098229 (NM). National Institutes of Health grant NS102417 (NM). National Institutes of Health grant NS123398 (NM). National Institutes of Health grant K22 NS123508 (KT). The Whole Brain Microscopy Facility was funded by award SCR\_017949 and the Zeiss AxioScanner 7 was funded by award 1S10OD032267-01.

## COMPETING INTERESTS

The authors declare no competing interests.

## ADDITIONAL INFORMATION

**Supplementary information** The online version contains supplementary material available at <https://doi.org/10.1038/s41435-026-00389-z>.

**Correspondence** and requests for materials should be addressed to Nancy L. Monson.

**Reprints and permission information** is available at <http://www.nature.com/reprints>

**Publisher's note** Springer Nature remains neutral with regard to jurisdictional claims in published maps and institutional affiliations.



**Open Access** This article is licensed under a Creative Commons Attribution-NonCommercial-NoDerivatives 4.0 International License, which permits any non-commercial use, sharing, distribution and reproduction in any medium or format, as long as you give appropriate credit to the original author(s) and the source, provide a link to the Creative Commons licence, and indicate if you modified the licensed material. You do not have permission under this licence to share adapted material derived from this article or parts of it. The images or other third party material in this article are included in the article's Creative Commons licence, unless indicated otherwise in a credit line to the material. If material is not included in the article's Creative Commons licence and your intended use is not permitted by statutory regulation or exceeds the permitted use, you will need to obtain permission directly from the copyright holder. To view a copy of this licence, visit <http://creativecommons.org/licenses/by-nc-nd/4.0/>.

© The Author(s) 2026